ACS APPLIED MATERIALS & INTERFACES

Subscriber access provided by CMU Libraries - http://library.cmich.edu

Article

Oxygen and nitrogen enriched 3D porous carbon for supercapacitors of high volumetric capacity

Jia Li, Kang Liu, Xiang Gao, Bin Yao, Kaifu Huo, Yongliang Cheng, Xiaofeng Cheng, Dongchang Chen, Bo Wang, Dong Ding, Meilin Liu, and Liang Huang

ACS Appl. Mater. Interfaces, **Just Accepted Manuscript** • Publication Date (Web): 19 Oct 2015

Downloaded from http://pubs.acs.org on October 19, 2015

Just Accepted

"Just Accepted" manuscripts have been peer-reviewed and accepted for publication. They are posted online prior to technical editing, formatting for publication and author proofing. The American Chemical Society provides "Just Accepted" as a free service to the research community to expedite the dissemination of scientific material as soon as possible after acceptance. "Just Accepted" manuscripts appear in full in PDF format accompanied by an HTML abstract. "Just Accepted" manuscripts have been fully peer reviewed, but should not be considered the official version of record. They are accessible to all readers and citable by the Digital Object Identifier (DOI®). "Just Accepted" is an optional service offered to authors. Therefore, the "Just Accepted" Web site may not include all articles that will be published in the journal. After a manuscript is technically edited and formatted, it will be removed from the "Just Accepted" Web site and published as an ASAP article. Note that technical editing may introduce minor changes to the manuscript text and/or graphics which could affect content, and all legal disclaimers and ethical guidelines that apply to the journal pertain. ACS cannot be held responsible for errors or consequences arising from the use of information contained in these "Just Accepted" manuscripts.

ACS Publications

ACS Applied Materials & Interfaces is published by the American Chemical Society.
1155 Sixteenth Street N.W., Washington, DC 20036

Published by American Chemical Society. Copyright © American Chemical Society. However, no copyright claim is made to original U.S. Government works, or works produced by employees of any Commonwealth realm Crown government in the course of their duties.

Oxygen and nitrogen enriched 3D porous carbon for supercapacitors of high volumetric capacity

Jia Li,‡[a] Kang Liu,‡[a] Xiang Gao,[a] Bin Yao,[a] Kaifu Huo,[a] Yongliang Cheng,[a] Xiaofeng Cheng,[a] Dongchang Chen,[b] Bo Wang,[a] Dong Ding,[b] Meilin Liu*[b] and Liang Huang* [a]

[a] Wuhan National Laboratory for Optoelectronics, School of Optical and Electronic Information, Huazhong University of Science and Technology, Wuhan 430074, Hubei, P. R. China

[b] School of Materials Science and Engineering, Georgia Institute of Technology, 771 Ferst Drive, Atlanta, Georgia 30332-0245, United States.

‡ Authors with equal contribution

Abstract: Efficient utilization and broader commercialization of alternative energies (e.g., solar, wind, and geothermal) hinges on the performance and cost of energy storage and conversion systems. For now and in the foreseeable future, the combination of rechargeable batteries and electrochemical capacitors remains the most promising option for many energy storage applications. Porous carbonaceous materials have been widely used as an electrode for batteries and supercapacitors. To date, however, the highest specific capacitance of an electrochemical double layer capacitor (EDLC) is only ~200 F/g, although a wide variety of synthetic approaches have been explored in creating optimized porous structures. Here we report our findings in synthesis of porous carbon through a simple, one-step process: direct carbonization of kelp in a NH_3 atmosphere at 700°C. The resulting oxygen and nitrogen enriched carbon has a three dimensional structure with specific surface area

greater than 1000 m^2/g. When evaluated as an electrode for electrochemical double layer capacitors, the porous carbon structure demonstrated excellent volumetric capacitance (>360 F/cm^3) with excellent cycling stability. This simple approach to low-cost carbonaceous materials with unique architecture and functionality could be a promising alternative to fabrication of porous carbon structures for many practical applications, including batteries and fuel cells.

Keywords: kelp, 3D porous carbon, energy storage, volumetric capacitance, long cycling stability

Introduction

Porous carbonaceous materials have been used in a wide variety of high-performance energy storage and conversion devices such as supercapacitors, lithium/sodium ion batteries, solar cells, and fuel cells,[1-6] owing to their large specific surface area, high electronic conductivity, excellent chemical stability, and minimum environmental impact. The tunable pore size may create accessible path for ionic transport, making porous carbon a favorable candidate for electrode materials of electrochemical capacitors (ECs).[7-11] Typically, carbonaceous materials with massive specific surface area can be activated in two ways, physical activation with different oxidizing atmosphere and chemical activation with KOH, H_3PO_4 or $ZnCl_2$.[1, 12-15] Recently, metal-organic frameworks, metal carbides, polymer precursors, and hard template-mediated synthesis have also been used to produce mesoporous carbonaceous structures.[16-20] Nevertheless, these methods still have

drawbacks, limiting their practical application because of the complicated fabrication processes and the high cost for scale-up. Direct pyrolysis of low-cost carbonaceous materials without an additional activation process could be a promising alternative to obtain porous carbon for practical application. [21-23]

Usually, pure carbon-based ECs store charge through electrochemical double layer effect on electrode surface (EDLCs). The performances of EDLCs mainly depend on both the accessible specific surface area and the pore structure of carbon electrode.[18, 20, 24, 25] In most cases, porous carbon-based ECs are known to suffer from ion-transport kinetics issues, resulting in a poor rate capability. [25] Carbonaceous materials with three dimensional (3D) ordered/aperiodic porous architecture facilitate ionic transport, therefore having a smaller resistance and shorter diffusion pathways.[26, 27] However, the highest specific capacitance of an electrochemical double layer capacitor is around 200 F/g, which limit the deliverable energy density. To improve the energy density of carbon-based capacitors, current researches are focusing on functionalizing carbon surface with oxygen and nitrogen functional groups to introduce fast redox reactions (pseudocapacitive behavior) on the surface of electrode.[28-31] To address these two sites, nitrogen or oxygen doped 3D porous carbon architecture hold great potential to fabricate advanced ECs.

Kelps are large seaweed (algae) belonging to the brown algae (phaeophyceae) in the order Laminariales. It has a high growth rate and abundant in sodium, potassium, calcium and magnesium, and has been widely

used as food product and source for industrial production of soda, glass and hydrocolloids. [32, 33] On the other hand, pyrolysis of carbonaceous materials in a NH_3 atmosphere is one of facile ways to obtain nitrogen doped carbon and to increase the specific surface area and pore volume of carbon materials simultaneously.[34] Here, we propose the synthesis of porous carbon through directly carbonizing kelp in the NH_3 atmospheres at 700°C. This oxygen and nitrogen enriched carbon shows fish-scale-like three dimensional structure with specific surface area over 1000 m^2/g. When evaluated as the electrode material for ECs, the porous carbon demonstrated exciting a volumetric capacitance over 360 F/cm^3 with excellent cycling stability.

Experimental

All the reagents used in the experiment were of analytical grade and used without further purification.

Synthesis of porous carbons: Kelp was purchased from Chinese supermarket without any other treatment. The kelp was carbonized in a tubular furnace with an ammonia or argon flow of 30 mL/min at 700 °C for 3 h under the heating rate of 3°C min^{-1}. The resulting black solid was then washed with 6 mol/LHCl and 6 mol/L KOH solutions for 12 h at 60 °C, respectively. The obtained black powder then washed with DI water several times and dried at 80 °C in the oven over night to get the 3 D porous carbons.

Preparation of the Electrodes. Unless otherwise specified, the electrodes were

composed of 80 wt. % 3D porous carbons powder, 10 wt% acetylene black (Alfa Aesar, 99.9%), and 10 wt% poly (tetrafluoroethylene) (PTFE) as a binder. The PTFE was dispersed in about 30 mL of ethanol before the addition of porous carbons and acetylene black. The resulting solution was homogenized by stirring overnight, and ethanol was evaporated in oil bath at 80°C until the formation of a rubber like paste, which was roll-pressed into a 20-μm-thick film on a flat glass surface. Roundness pieces of film, typically of 1 cm^2 surface area and about 1 mg mass. Before electrochemical characterization, the electrodes were dried overnight at 60 °C and were subsequently immersed in the electrolyte solution for 0.5 h in order to enhance the electrolyte diffusion into the material bulk.

Physical and Electrochemical Characterization. The microstructural properties of electrode materials were characterized by X-ray diffraction using the Cu Kα radiation (λ = 1.5418 Å) (XRD, Philips X' Pert Pro), field-emission SEM (FE-SEM, FEI Nova 450 Nano), TEM (HRTEM, TECNAI, Titan) equipped with an energy-dispersive X-ray spectroscopy (EDAX) detector, X-ray photoelectron spectroscope (XPS, AXIS-ULTRA DLD-600W). The electrochemical properties of the products were investigated with cyclic voltammetry (CV) and chronopotentiometry measurements employing an EC-lab, and the electrochemical impedance spectroscopy (EIS) were measured by an Autolab PGSTAT302N at a frequency ranging from 100 mHz to 10 kHz with a potential amplitude of 10 mV. All the testing was conducted in the "Swagleok" cell. The two electrode system was assembled with two KCN-700 electrodes and one separator constructing sandwich

structure. The mass of electrode materials were measured by a microbalance (CPA225D, Sartorius) with an accuracy of 0.01 mg. N2 adsorption-desorption isotherms were performed on a Micrometrics ASAP 2000. Four-probe configuration electrical resistively was tested by a standard four-probe configuration (RTS-8) and the tested samples were prepared according the following process: Firstly, ~0.5 g porous carbons power were dried at 80 °C for 12 h; Then the power was pressed under a force of approximately 4 KPa by a table press machine (yp-180, Xingye). Infrared spectroscopy (IR) analysis of the materials was performed on a VERTEX 70 (Bruker) Fourier transformation infrared spectrometer over the wave number range of 400 ~ 4000 cm^{-1} with KBr pelletisation. Raman analysis was performed on a LabRAM HR800 (Horiba JobinYvon) with a 532 nm illuminant.

Results and Discussion

Kelp was purchased from the manufacturer of Jiaxingda in Wuhan without any further treatment. The surface of the kelp displays a leaf-like structure under a scanning electron microscope (SEM). (Figure 1a inset2) The porous carbon was fabricated by carbonizing kelp in the NH_3 atmospheres at 700°C, namely KCN-700. (Figure 1a) The porous carbon produced by pyrolysis of kelp in an argon atmosphere at 700°C is called KCA-700, which is compared with KCN-700. The detailed morphology and structural features of KCN-700 were characterized by SEM and transmission electron microscope (TEM). Surprisingly, as shown in Figure 1b, the surface of KCN-700 consists of multiple oriented porous carbon piles showing 3D architecture. (Figure 1c,

1e) The mesoporous structure could be observed more clearly in the TEM image. The porosity is made up of randomly oriented narrow pores, thereby anticipating the results obtained from the nitrogen physisorption measurement. (Figure 1d) High-resolution TEM revealed highly disordered porous carbon structure without graphite ribbons and crystalline impurities. (Figure 1d inset)

X-ray diffraction (XRD) was employed to investigate the crystallographic structure of the as-prepared samples. As shown in Figure S1a (supporting information), the XRD patterns contain two broad peaks located at 24.5° and 43.6° corresponding to the (002) and (100) reflection of carbon materials, respectively, representing a disorder phase in the samples. Further, Raman spectroscopy was also used to elucidate the nature of the samples. (Figure S1b,) Two characteristic peaks at 1349 cm^{-1} and 1597 cm^{-1} are assigned to the breathing mode of κ-point phonons of A_{1g} symmetry (D band) and the in-plane stretching motion of symmetric sp^2 C-C bonds (G band).[35] [32-34] The degree of disorder of the carbon material can be generally described by the ratio of the intensity of D and G band. In our work, the integrated intensities I_D: I_G ratio of KCA-700 and KCN-700 numerically equal to 1.11 and 1.07, respectively, indicating the existence of considerable structural disorder in the carbon matrix, consistent with the HRTEM observation and XRD analysis results.

The nitrogen adsorption/desorption isotherms of the porous carbon showed significant impact of the activation atmosphere on their porosity. As shown in the Figure 2a, N_2 adsorption and desorption isotherms of KCN-700 at low

relative pressure indicated the existence of a number of micropores. For KCN-700, the total amount of N_2 adsorbed at $P/P_0 \approx 0.99$ is around 400 cm^3/g, which corresponds to the moderately pore volume of 0.62 cm^3/g. The total BET (Brunauer–Emmett–Teller) specific surface area (SSA) of KCN-700 was found to be 1002.6 m^2/g, which is higher than SSA of KCA-700 (677.5 m^2/g), suggesting the activation effect of NH_3. According to non-local density functional theory (NL-DFT) calculations, the two samples have hierarchical porous structure with the pore size ranging from 1.5 to 92 nm. (Figure 2b) The X-ray photoelectron spectrometer (XPS) was used to identify the elemental composition of the porous carbons obtained under different atmosphere. As a reference, KCA-700 consists of 94.69 at% carbon, 3.16 at% oxygen and 2.15 at% nitrogen, suggesting an effective carbonization. After the activation under NH_3, the nitrogen content has a significant enhancement (N, 5.04 at%) as expected at the pyrolsis temperature of 700°C. Moreover, the oxygen content in the KCN-700 (O, 8.76 at%) also increased obviously, which should be due to the reaction of NH_3 with oxygenated species therefore restricting the decomposition carboxyl group to CO_2. (Table. S1, FigureS2)The high resolution XPS spectra of N 1s and O 1s were collected to understand the formed N-carbon and O-carbon bonding under NH_3. Nitrogen atoms were found in three different contributions in the carbon matrix: pyridinic N (N-1, 398.5 eV), pyrrolic-N (N-2, 400.3 eV), and pryridine-N-oxide (N-4, 403.5 eV). (Figure 2c) The oxygen functionalities found for KCN-700 after deconvolution

of the O1s peaks are carbonyl oxygen of Keto and quinone (O1, 531.5 eV), non-carbonyl (ether-type) oxygen atoms in esters and anhydrides (O2, 533.1 eV), and oxygen atoms in carboxylic groups (O3, 534.5 eV).[29, 36, 37] (Figure 2d) These abundant oxygen and nitrogen functional groups on the surface of ACs couple with high specific surface area offer a strong tendency to deliver exciting electrochemical performance.[38]

We then investigate the electrochemical properties of the ACs in a three-electrode cell with 6 M KOH electrolyte using cyclic voltammetry (CV) and Galvanostatic charge-discharge（GCD）. The typical CV curves of KCN-700 display rectangular shape as well as triangular GCD profiles demonstrate the reversible capacitive behavior. (Figure 3a-b) More importantly, the CV curves of KCN-700 still maintain a rectangular shape even at a sweep rate of 500 mV/s, implying remarkable high performance under high rate operation. The rectangular CV profile at higher sweep rate is based on the presence of mesopores. The hydrated cation (K^+) and anion (OH^-) in KOH solution which have ion dimensions of 0.33 and 0.3 nm respectively may easily diffuse through the pores size under 1 nm.[39] Moreover, the CV curve of KCN-700 at sweep rates of 50 mV/s has a much larger integral area than the that of KCA-700 at same sweep rate, revealing the better specific capacitance. (Figure 3c) Electrochemical impedance spectroscopy measurement was also conducted to evaluate the difference of electrochemical activity of KCN-700 and KCA-700. (Figure S4) The smaller diameter of the semicircle of KCN-700

reveals the less charge-transfer resistance on the electrode surface than KCA-700. A much higher slope at the low-frequency region clearly shows the a better pore accessibility for electrolyte ions for KCN-700 than KCA-700, which is ascribed to higher amount of nitrogen and oxygen functional groups which may enhance the wettability of the KCN-700. The GCD measurements were performed with different current densities to assess the specific capacitance. As described in the Fig. 3c, KCN-700 also demonstrated the better capacitive behavior compare to the KCA-700, consistent with CV testing. The maximum specific capacitance is calculated to be 440 F/g at the current density of 0.5 A/g, with a capacitance of 180 F/g at a higher current density of 150 A/g. (Figure 3d) This high capacitance performance under such high rate mainly attribute to the unique three dimensional structure with high surface area which may create an efficient electron percolation path as well as effective electrolyte access to the electrochemically active materials without limiting charge transport. Besides surface area, the pore size distribution of carbon material also plays an important role in the charge storage. The hierarchical porous structure favors rapid ionic diffusion from mesopore/macropore to the micropore, resulting in fast transportation of electrolyte ions through the whole architecture and sufficient reaction with the nitrogen or oxygen functionalities which offer massive pseudocapacitive behavior. Moreover, these mesopores could act as channels for electrolyte ions to access the inner micropores and enhance accessible surface area.

Besides gravimetric specific capacitance, the volumetric capacitance is one of crucial criteria to evaluate the performance of the SCs system.[40-42] It can be calculated based on the following equation:

$$C_v = C_g \cdot \rho$$

where C_v is the volumetric capacitance, C_g is the gravimetric capacitance and ρ is the particle density.[29, 43-47] According to the mass density of KCN-700 electrode (roughly 0.82 g/cm^3), the volumetric capacitance could achieve 360 F/cm^3, which is comparable to the highest value of carbon electrode based on the oxygen functionalized graphene.[48] (Figure 3e)

The cycling stability of this electrode in the KOH electrolyte was conducted under the sweep rate of 50 mV/s. As described in Figure 1, even after 15000 cycles, the capacitance retention still retain around 95.4%, indicating the strong architecture of the three dimensional structure and superior stability nitrogen or oxygen functional group. (Figure 3f)

As described in the previous report, carbon-based material have a wide operation voltage window even over 2V in the neutral electrolyte, effectively improving the deliverable energy density of SCs.[49, 50] In order to evaluate the potential practical application of KCN-700, the symmetric supercapacitor was assembled using 1 M Na_2SO_4 aqueous solution electrolyte. As shown in the Figure 4a, the CV curves at a sweep rate of 50 mV/s with voltage window adjusted in the range from 0.8 to 2 V did not reveal any significant increase of

anodic current. CV profiles at different sweep rates from 20 mV/s to 200 mV/s were presented in the Figure 1. Even at a high sweep rate of 200 mV/s, the CV curve still shows a rectangular-like shape, indicating ideal capacitive behavior. (Figure S5) As the most important parameter for SCs, the Ragone plot of the symmetric SCs KCN-700// KCN-700 were shown in the Figure 1 based on the following equations:

$$E = 0.5\ CV^2$$

$$P = E/t$$

Where E and P are energy density and power density of the SCs, respectively. C (F/ g) is the capacitance of the SCs, V is the operating voltage (V), and t is the discharge time (s) respectively. This KCN-700 based SCs exhibit an impressive energy density of 28.8 Wh/kg, which is superior than most of previous reported carbonaceous electrode in aqueous electrolyte.[51, 52 43, 48, 53] Additionally, even at a high power density of 14.4 kW/kg, the cell also delivers an energy density of 14.4 kg/ Wh. (Figure 4b) According to the transformation of volumetric capacitance and gravimetric capacitance, the cell owns a ultrahigh volumetric energy density of 23.6 mWh/ L， which is comparable to most carbon materials reported in aqueous electrolytes.[33, 43, 44, 48, 52, 54-57] (Figure 4c) The stability of this cell was evaluated by long-term CV cycling at a sweep rate of 50 mV/s in the voltage window of 1.8 V. It can be seen that the capacitance retention retains 92.3% of its initial capacitance after 10000 cycles, proving the superb robustness of the KCN-700. Thereby, taking into account

cost-effective and scalable characteristics coupled with remarkable specific capacitance and stability, the mesoporous KCN-700 hold great significance for both academic and industry communities. (Figure 4d)

Conclusions

In summary, we have presented a facile approach to produce 3D mesoporous carbon through directly carbonizing kelp in a NH_3 atmosphere. This porous structure contains large amount of nitrogen and oxygen functional groups, around 5.04 and 8.76%, respectively, while possessing a high surface area over 1000 g/ m^2. These unique structural properties allow short ionic diffusion paths and consequently rapid transport of ions throughout the carbonaceous matrix, leading to ultrahigh volumetric capacitance (over 360 F/ cm^3), excellent cycling stability, and remarkable volumetric energy density (around 23.6 mWh/L). All the results indicate that the development of facile, cost-effective, and scalable synthesis route to produce porous 3D carbon materials is well-suited for construction of high-performance ECs.

AUTHOR INFORMATION

* Corresponding author.

E-mail: huangliang421@hust.edu.cn and meilin.liu@mse.gatech.edu

Acknowledge

This work was financially supported by the China Postdoctoral Science Foundation (Project No.2014M550390, 2014M552033), the Heterogeneous Functional Materials (HetroFoaM) Center, an Energy Frontier Research Center funded by the U.S. Department of Energy, Office of Science, Office of Basic Energy Sciences under Award Number DE-SC0001061.

Supporting Information

This material is available free of charge via the Internet at http://pubs.acs.org. The XRD, Raman spectra and more electrochemical characteristics of KCN-700 are listed in the support information.

References

(1) Sevilla, M.; Mokaya, R. Energy Storage Applications of Activated Carbons: Supercapacitors and Hydrogen Storage. *Energy Environ. Sci.* **2014**, *7*, 1250-1280.

(2) Navarro, R. M., Peña, M. A.; Fierro, J. L. G. Hydrogen Production Reactions from Carbon Feedstocks: Fossil Fuels and Biomass. *Chem. Rev.* **2007**, *107*, 3952-3991.

(3) Gür, T. M. Critical Review of Carbon Conversion in "Carbon Fuel Cells". *Chem. Rev.* **2013**, *113*, 6179-6206.

(4) McCreery, R. L. Advanced Carbon Electrode Materials for Molecular Electrochemistry, *Chem. Rev.* **2008**, *108*, 2646-2687.

(5) Titirici, M.-M., White, R. J., Brun, N., Budarin, V. L., Su, D. S., del Monte, F., Clark, J. H.; MacLachlan, M. J. Sustainable Carbon Materials, *Chem. Soc. Rev.* **2015**, *44*, 250-290.

(6) Ma, T.-Y., Liu, L.; Yuan, Z. Y. Direct Synthesis of Ordered Mesoporous Carbons, *Chem. Soc. Rev.* **2013**, *42*, 3977-4003.

(7) Chmiola, J., Largeot, C., Taberna, P. L., Simon, P., Gogotsi, Y. Monolithic Carbide-Derived Carbon Films for Micro-Supercapacitors, *Science.* **2010**, *328*, 480-483.

(8) Zhu, Y., Murali, S., Stoller, M. D., Ganesh, K. J., Cai, W., Ferreira, P. J., Pirkle A., Wallace, R. M., Cychosz, K. A., Thommes, M., Su, D., Stach, E. A., Ruoff, R. S., Carbon-Based Supercapacitors Produced by Activation of Graphene, *Science.* **2011**, *332*, 1537-1541.

(9) Zhao, J., Lai, H. W., Lyu, Z. Y., Jiang, Y. F., Xie, K., Wang, X. Z., Wu, Q., Yang, L. J., Jin, Z., Ma, Y. W., Liu, Jie., Hu, Z., Hydrophilic Hierarchical Nitrogen-Doped Carbon Nanocages for Ultrahigh Supercapacitive Performance, *Adv. Mater*. **2015**, *27*, 3541–3545.

(10) Hou, J., Cao, C., Idrees, F.; Ma, X. Hierarchical Porous Nitrogen-Doped Carbon Nanosheets Derived from Silk for Ultrahigh-Capacity Battery Anodes and Supercapacitors, *ACS Nano.* **2015**, *9*, 2556–2564.

(11) White, R. J., Budarin, V., Luque, R., Clark, J. H.; Macquarrie, D. J. Tuneable Porous Carbonaceous Materials From Renewable Resources, *Chem. Soc. Rev.* **2009**, *38*, 3401-3418.

(12) Borchardt, L., Hoffmann, C., Oschatz, M., Mammitzsch, L., Petasch, U., Herrmann, M.; Kaskel, S. Preparation and Application of Cellular and Nanoporous Carbides. *Chem. Soc. Rev.* **2012**, *41*, 5053-5067.

(13) Fan, X., Yu, C., Yang, J., Ling, Z., Hu, C., Zhang, M.; Qiu, J. A Layered-Nanospace-Confinement Strategy for the Synthesis of Two-Dimensional Porous Carbon Nanosheets for High-Rate Performance Supercapacitors. *Adv. Energy Mater.* **2014**, *5*, 1401761-1401767.

(14) Han, X., Funk, M. R., Shen, F., Chen, Y.-C., Li, Y., Campbell, C. J., Dai, J., Yang, X., Kim, J.-W., Liao, Y., Connell, J. W., Barone, V., Chen, Z., Lin, Y.; Hu, L., Scalable Holey Graphene Synthesis and Dense Electrode Fabrication toward High-Performance Ultracapacitors. *ACS Nano.* **2014**, *8*, 8255–**8265**.

(15) Xu, Y., Lin, Z., Zhong, X., Huang, X., Weiss, N. O., Huang, Y.; Duan, X. Holey Graphene Frameworks for Highly Efficient Capacitive Energy Storage. *Nat commun.* **2014**, *5*, 4554.

(16) Zhang, W., Wu, Z.-Y., Jiang, H. L.; Yu, S. H. Nanowire-Directed Templating Synthesis of Metal–Organic Framework Nanofibers and Their Derived Porous Doped Carbon Nanofibers for Enhanced Electrocatalysis. *J. Am. Chem. Soc.* **2014**, *136*, 14385–14388.

(17) Li, Z., Wu, D., Liang, Y., Fu, R.; Matyjaszewski, K. Synthesis of Well-Defined Microporous Carbons by Molecular-Scale Templating with Polyhedral Oligomeric Silsesquioxane Moieties, *J. Am. Chem. Soc.* **2014**, *136*, 4805-4808.

(18) Chmiola, J., Yushin, G., Gogotsi, Y., Portet, C., Simon, P.; Taberna, P. L. Anomalous Increase in Carbon Capacitance at Pore Sizes Less Than 1 Nanometer, *Science* **2006**, *313*, 1760-1763.

(19) Han, S., Sohn, K.; Hyeon, T. Fabrication of New Nanoporous Carbons through Silica Templates and Their Application to the Adsorption of Bulky Dyes. *Chem. Mater.* **2000**, *12*, 3337-3341.

(20) Nishihara, H.; Kyotani, T. Templated Nanocarbons for Energy Storage. *Adv. Mater.* **2012**, *24*, 4473-4498.

(21) Biswal, M., Banerjee, A., Deo, M.; Ogale S. From Dead Leaves to High Energy Density Supercapacitors. *Energy Environ. Sci.* **2013**, *6*, 1249-1259.

(22) Dutta, S., Bhaumik, A.; Wu, K. C. W. Hierarchically Porous Carbon Derived from Polymers and Biomass: Effect of Interconnected Pores on Energy Applications. *Energy Environ. Sci.* **2014**, *7*, 3574-3592.

(23) Wu, X. L., Wen, T., Guo, H. L., Yang, S., Wang, X.; Xu, A.W. Biomass-Derived Sponge-like Carbonaceous Hydrogels and Aerogels for Supercapacitors. *ACS Nano* **2013**, *7*, 3589-3597.

(24) Taberna, P. L., Simon, P.; Fauvarque, J. F. Electrochemical Characteristics and Impedance Spectroscopy Studies of Carbon-Carbon Supercapacitors. *J. Electrochem. Soc.* **2003**, *150*, A292-A300.

(25) Portet, C., Yushin, G.; Gogotsi, Y. Effect of Carbon Particle Size on Electrochemical Performance of EDLC. *J. Electrochem. Soc.* **2008**, *155*, A531-A536.

(26) Wang, D. W., Li, F., Liu, M., Lu, G. Q.; Cheng, H. M. 3D Aperiodic Hierarchical Porous Graphitic Carbon Material for High-Rate Electrochemical Capacitive Energy Storage. *Angew. Chem., Int. Ed.* **2008**, *47*, 373-376.

(27) Sevilla, M.; Fuertes, A. B. Direct Synthesis of Highly Porous Interconnected Carbon Nanosheets and Their Application as High-Performance Supercapacitors. *ACS Nano* **2014**, *8*, 5069-5078.

(28) Su, F., Poh, C. K., Chen, J. S., Xu, G., Wang, D., Li, Q., Lin, J.; Lou, X. W. Nitrogen-containing Microporous Carbon Nanospheres with Improved Capacitive Properties. *Energy Environ. Sci.* **2011**, *4*, 717-724.

(29) Seredych, M., Hulicova-Jurcakova, D., Lu, G. Q.; Bandosz, T. J. Surface functional Groups of Carbons and the Effects of Their Chemical Character, Density and Accessibility to Ions on Electrochemical Performance. *Carbon* **2008**, *46*, 1475-1488.

(30) Cheng, Y. L., Huang, L., Xiao, X., Yao B., Yuan, L. Y., Li, T. Q., Hu, Z. M., Wang, B., Wan, J., Zhou, J. Flexible and Cross-linked N-doped Carbon Nanofiber Network for High Performance Freestanding Supercapacitor Electrode, *Nano Energy*, **2015**, *15*, 66–74.

(31) Hulicova-Jurcakova, D., Kodama, M., Shiraishi, S., Hatori, H., Zhu, Z. H.; Lu, G. Q., Nitrogen-Enriched Nonporous Carbon Electrodes with Extraordinary Supercapacitance. *Adv. Funct. Mater.* **2009**, *19*, 1800-1809.

(32) Marinho-Soriano, E., Fonseca, P. C., Carneiro, M. A. A.; Moreira, W. S. C. Seasonal Variation in the Chemical Composition of Two tropical Seaweeds. *Bioresour. Technol.* **2006**, *97*, 2402-2406.

(33) Raymundo-Piñero, E., Cadek, M.; Béguin, F., Tuning Carbon Materials for Supercapacitors by Direct Pyrolysis of Seaweeds. *Adv. Funct. Mater.* **2009**, *19*, 1032-1039.

(34) Luo, W., Wang, B., Heron, C. G., Allen, M. J., Morre, J., Maier, C. S., Stickle, W. F.; Ji, X. Pyrolysis of Cellulose under Ammonia Leads to Nitrogen-Doped Nanoporous Carbon Generated through Methane Formation, *Nano Letters* **2014**, *14*, 2225-2229.

(35) Sadezky, A., Muckenhuber, H., Grothe, H., Niessner, R.; Pöschl, U. Raman Microspectroscopy of Soot and Related Carbonaceous Materials: Spectral Analysis and Structural Information. *Carbon* **2005**, *43*, 1731-1742.

(36) Jackson, S. T.; Nuzzo, R. G. Determining Hybridization Differences for Amorphous Carbon From the XPS C 1s envelope. *Appl. Surf. Sci.* **1995**, *90*, 195-203.

(37) Chaikittisilp, W., Hu, M., Wang, H., Huang, H. S., Fujita, T., Wu, K. C. W., Chen, L. C., Yamauchi, Y.; Ariga K. Nanoporous Carbons through direct Carbonization of a Zeolitic Imidazolate Framework for Supercapacitor electrodes. *Chem. Commun.* **2012**, *48*, 7259-7261.

(38) Wang, D. W., Li, F., Yin, L. C., Lu, X., Chen, Z. G., Gentle, I. R., Lu, G. Q.; Cheng, H. M. Nitrogen-Doped Carbon Monolith for Alkaline Supercapacitors and Understanding Nitrogen-Induced Redox Transitions, *Chem. - Eur. J.* **2012**, *18*, 5345-5351.

(39) Nightingale, E. R. Phenomenological Theory of Ion Solvation. Effective Radii of Hydrated Ions. *J. Phys. Chem.* **1959**, *63*, 1381-1387.

(40) Yu, G., Xie, X., Pan, L., Bao, Z.; Cui, Y. Hybrid Nanostructured Materials for High-Performance Electrochemical Capacitors. *Nano Energy.* **2013**, *2*, 213-234.

(41) Gogotsi, Y.; Simon, P. True Performance Metrics in Electrochemical Energy Storage. *Science.* **2011**, *334*, 917-918.

(42) Yang, X., Cheng, C., Wang, Y., Qiu, L.; Li, D. Liquid-Mediated Dense Integration of Graphene Materials for Compact Capacitive Energy Storage. *Science.* **2013**, *341*, 534-537.

(43) Long, C., Chen, X., Jiang, L., Zhi, L.; Fan, Z. Porous Layer-stacking Carbon Derived From In-built Template in Biomass For High Volumetric Performance Supercapacitors. *Nano Energy.* **2015**, *12*, 141-151.

(44) Tao, Y., Xie, X., Lv, W., Tang, D. M., Kong, D., Huang, Z., Nishihara, H., Ishii, T., Li, B., Golberg, D., Kang, F., Kyotani, T.; Yang, Q. H. Towards Ultrahigh Volumetric Capacitance: Graphene Derived Highly Dense but Porous Carbons for Supercapacitors. *Sci. Rep.* **2013**, *3*, 2975.

(45) Laušević, Z., Apel, P. Y., Krstić, J. B.; Blonskaya, I. V. Porous Carbon Thin Films for Electrochemical Capacitors, *Carbon.* **2013**, *64*, 456-463.

(46) Xia, K., Gao, Q., Jiang, J.; Hu, J. Hierarchical Porous Carbons with Controlled Micropores and Mesopores for Supercapacitor Electrode Materials. *Carbon* **2008**, *46*, 1718-1726.

(47) Yan, J., Wei, T., Shao, B., Ma, F., Fan, Z., Zhang, M., Zheng, C., Shang, Y., Qian, W.; Wei, F. Electrochemical Properties of Graphene Nanosheet/Carbon Black Composites as Electrodes for Supercapacitors. *Carbon.* **2010**, *48*, 1731-1737.

(48) Yan, J., Wang, Q., Wei, T., Jiang, L., Zhang, M., Jing, X.; Fan, Z. Template-Assisted Low Temperature Synthesis of Functionalized Graphene for Ultrahigh Volumetric Performance Supercapacitors. *ACS Nano.* **2014**, *8*, 4720-4729.

(49) Fic, K., Lota, G., Meller, M.; Frackowiak, E. Novel Insight Into Neutral Medium as Electrolyte for High-voltage Supercapacitors. *Energy Environ. Sci.* **2012**, *5*, 5842-5850.

(50) Bichat, M. P., Raymundo-Piñero, E.; Béguin, F. High Voltage Supercapacitor Built with Seaweed Carbons in Neutral Aqueous Electrolyte. *Carbon.* **2010**, *48*, 4351-4361.

(51) Puthusseri, D., Aravindan, V., Madhavi, S.; Ogale, S. 3D Micro-porous Conducting Carbon Beehive by Single Step Polymer Carbonization for High Performance Supercapacitors: the Magic of in Situ Porogen Formation. *Energy Environ. Sci.* **2014**, *7*, 728-735.

(52) Raymundo-Piñero, E., Leroux, F.; Béguin, F. A High-Performance Carbon for Supercapacitors Obtained by Carbonization of a Seaweed Biopolymer. *Adv. Mater.* **2006**, *18*, 1877-1882.

(53) Wang, X., Zhang, Y., Zhi, C., Wang, X., Tang, D., Xu, Y., Weng, Q., Jiang, X., Mitome, M., Golberg, D.; Bando, Y. Three-dimensional Strutted Graphene Grown by Substrate-free Sugar Blowing for High-power-density Supercapacitors. *Nat commun.* **2013**, *4*, 2905.

(54) Zhang, J., Jiang, J., Li, H.; Zhao, X. S. A High-performance Asymmetric Supercapacitor Fabricated with Graphene-based Electrodes. *Energy Environ. Sci.* **2011**, *4*, 4009-4015.

(55) Chen, L. F., Zhang, X. D., Liang, H. W., Kong, M., Guan, Q. F., Chen, P., Wu, Z. Y.; Yu, S. H. Synthesis of Nitrogen-Doped Porous Carbon Nanofibers as an Efficient Electrode Material for Supercapacitors. *ACS Nano.* **2012**, *6*, 7092-7102.

(56) Hu, J., Kang, Z., Li, F.; Huang, X. Graphene with Three-dimensional Architecture for High Performance Supercapacitor. *Carbon.* **2014**, *67*, 221-229.

(57) Xiao, N., Tan, H., Zhu, J., Tan, L., Rui, X., Dong, X.; Yan, Q. High-Performance Supercapacitor Electrodes Based on Graphene Achieved by Thermal Treatment with the Aid of Nitric Acid. *ACS Appl. Mater. Interfaces.* **2013**, *5*, 9656-9662.

FIGURE CAPTIONS

Figure 1. (a) The schematic of carbonization process of kelp in the NH_3, inset is Kelp (1), SEM images of Kelp (2) and activated carbon powder (3); (b) SEM image of KCN-700, inset is image of fish; (c) high magnification SEM image of KCN-700; (d) TEM image of KCN-700; (e) schematic of electrolyte ionic transportation through KCN-700 porous 3D structure.

Figure 2. (a) N_2 adsorption and desorption isotherms of KCN-700 and KCA-700; (b) pore size distribution of KCN-700 and KCA-700; (c)N_{1s} and (d) O_{1s} XPS profiles of KCN-700 and KCA-700.

Figure 3. (a) CV curves of KCN-700 at various sweep rates; (b) CDG profiles of KCN-700 with different current densities; (c) CV curves of KCN-700 and KCA-700 at 50 mV/s; (d) Specific capacitances of KCN-700 and KCA-700; (e) Comparison of the maximum volumetric and gravimetric capacitances KCN-700 electrode with other carbon electrodes (maximum value) in aqueous electrolyte; (f) Cycling stabilities of KCN-700 and KCA-700 at the sweep rate of 50mV/s.

Figure 4. (a) CV curves KCN-700//KCN-700 symmetric capacitor at a scan rate of 50 mV/s in different voltage windows; (b) Ragone plots of KCN-700 and other carbon-based symmetric supercapacitors; (c) Comparison of the volumetric and gravimetric energy densities of different symmetric supercapacitors using carbon-based electrode materials in aqueous electrolytes. (d) Cycling stability of the symmetric supercapacitor within 10 000 cycles at a scan rate of 50 mV/s. The inset shows the CV curves with the selected cycles.

Figures 1.

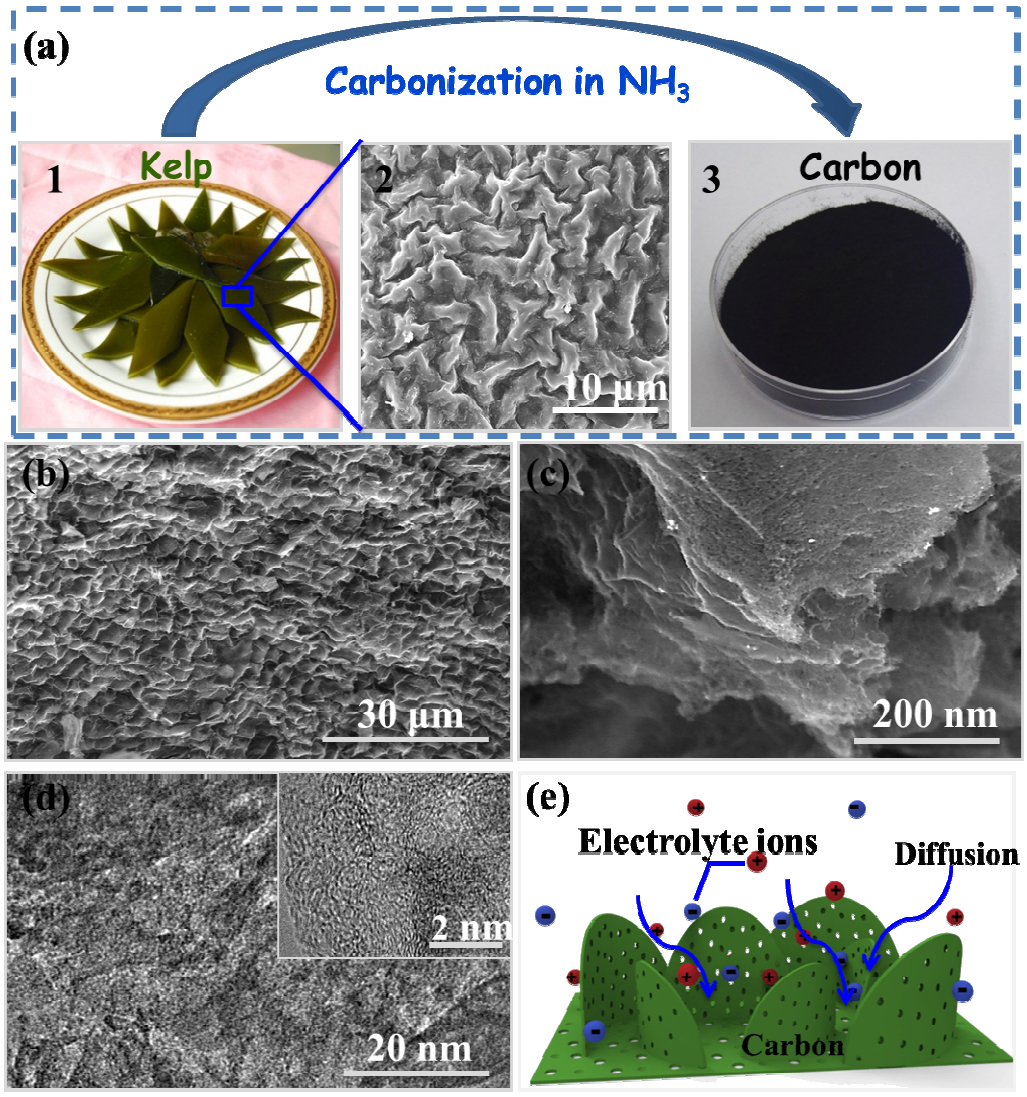
(a)
Carbonization in NH_3
1
Kelp
2
10 μm
3
Carbon
(b)
30 μm
(c)
200 nm
(d)
2 nm
20 nm
(e)
Electrolyte ions
Diffusion
Carbon

Figure 2.

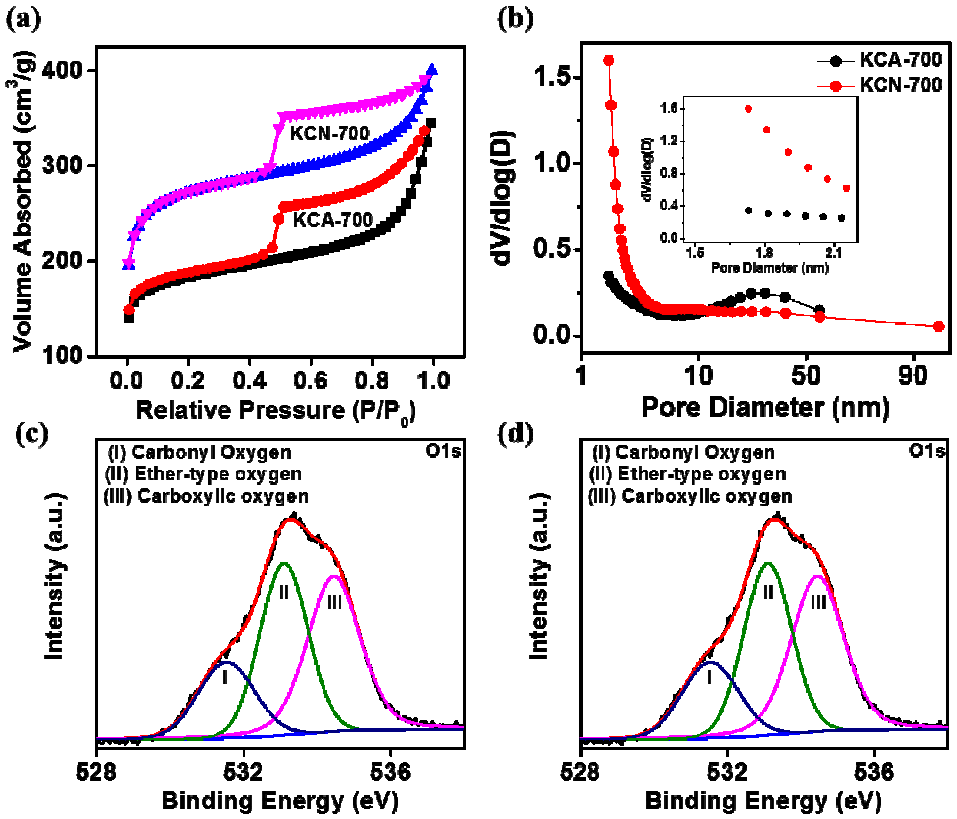
(a)
Volume Absorbed (cm3/g)
KCN-700
KCA-700
Relative Pressure (P/P0)
(b)
KCA-700
KCN-700
dV/dlog(D)
Pore Diameter (nm)
(c)
(I) Carbonyl Oxygen
(II) Ether-type oxygen
(III) Carboxylic oxygen
O1s
Intensity (a.u.)
Binding Energy (eV)
(d)
(I) Carbonyl Oxygen
(II) Ether-type oxygen
(III) Carboxylic oxygen
O1s
Intensity (a.u.)
Binding Energy (eV)

Figure 3.

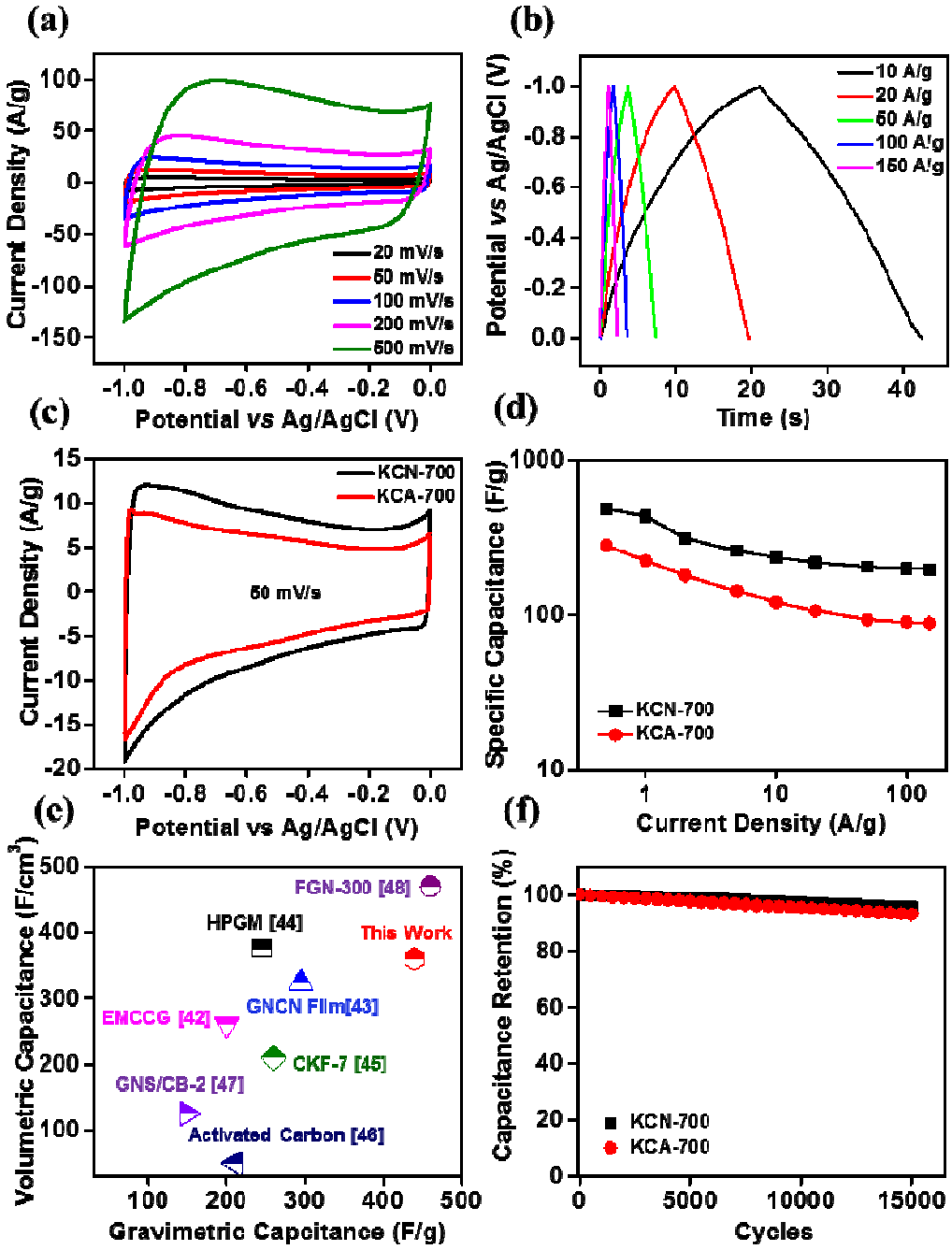
(a)
Current Density (A/g)
Potential vs Ag/AgCl (V)
20 mV/s
50 mV/s
100 mV/s
200 mV/s
500 mV/s
(b)
Potential vs Ag/AgCl (V)
Time (s)
10 A/g
20 A/g
50 A/g
100 A/g
150 A/g
(c)
Current Density (A/g)
Potential vs Ag/AgCl (V)
KCN-700
KCA-700
50 mV/s
(d)
Specific Capacitance (F/g)
Current Density (A/g)
KCN-700
KCA-700
(e)
Volumetric Capacitance (F/cm3)
Gravimetric Capacitance (F/g)
FGN-300 [48]
HPGM [44]
This Work
GNCN Film[43]
EMCCG [42]
CKF-7 [45]
GNS/CB-2 [47]
Activated Carbon [46]
(f)
Capacitance Retention (%)
Cycles
KCN-700
KCA-700

Figure 4.

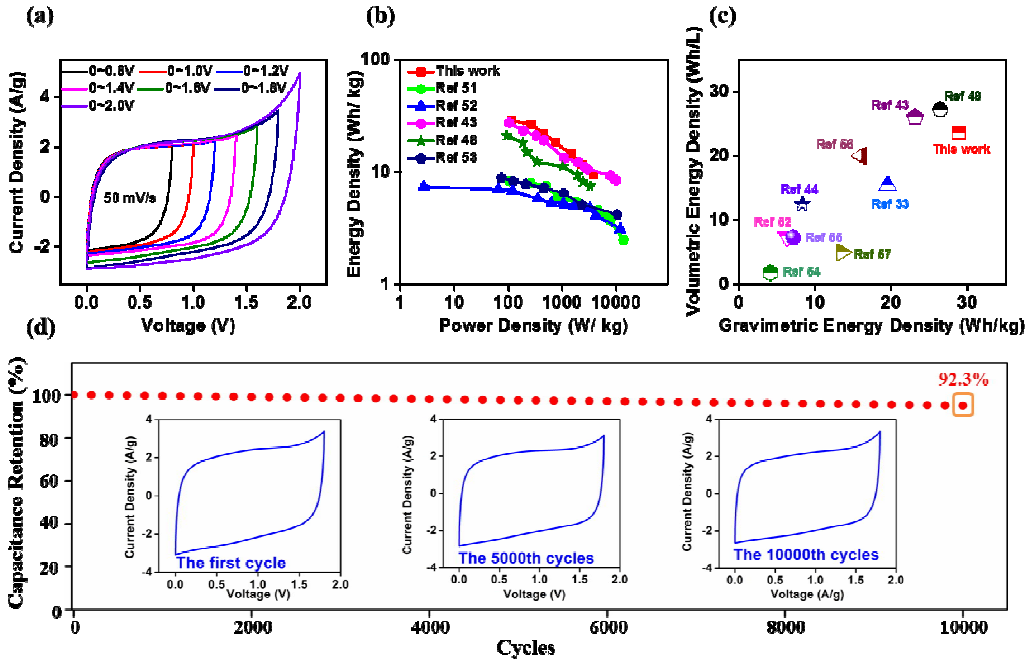
(a)
0~0.8V
0~1.0V
0~1.2V
0~1.4V
0~1.6V
0~1.8V
0~2.0V
50 mV/s
Current Density (A/g)
Voltage (V)
(b)
This work
Ref 51
Ref 52
Ref 43
Ref 48
Ref 53
Energy Density (Wh/ kg)
Power Density (W/ kg)
(c)
Ref 43
Ref 49
This work
Ref 58
Ref 44
Ref 33
Ref 62
Ref 66
Ref 67
Ref 64
Volumetric Energy Density (Wh/L)
Gravimetric Energy Density (Wh/kg)
(d)
92.3%
The first cycle
The 5000th cycles
The 10000th cycles
Capacitance Retention (%)
Cycles

TOC graphic

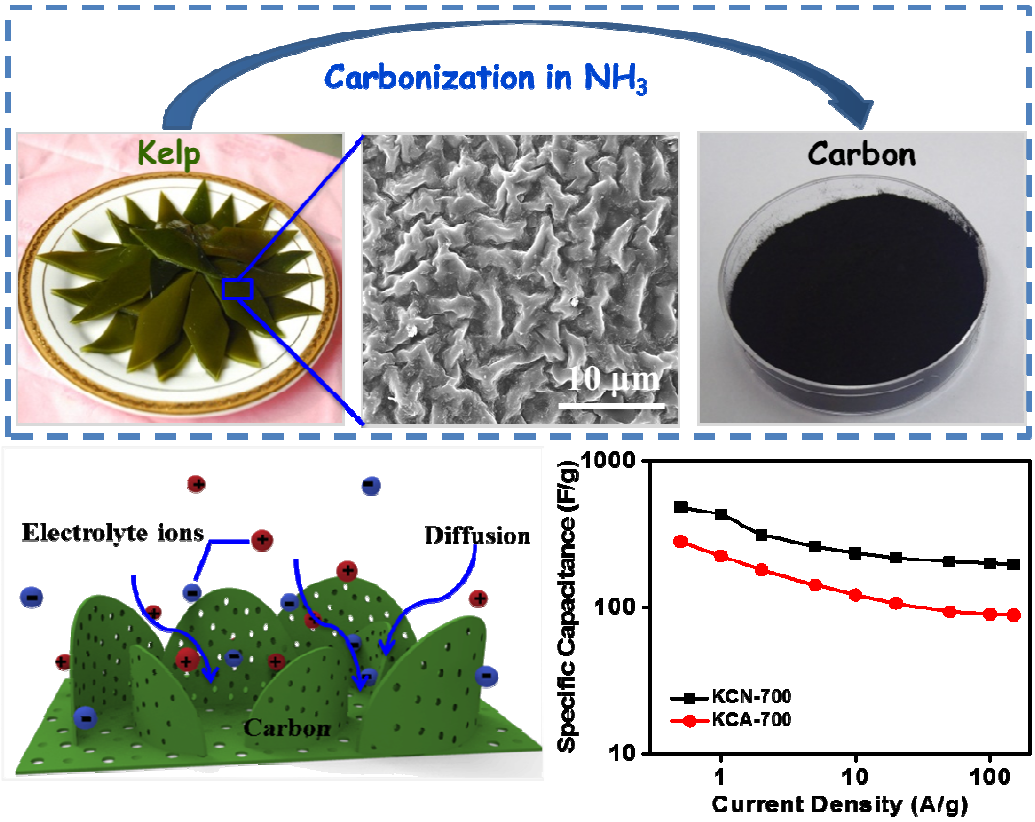
Carbonization in NH_3
Kelp
10 μm
Carbon
Electrolyte ions
Diffusion
Carbon
Specific Capacitance (F/g)
1000
100
10
KCN-700
KCA-700
1
10
100
Current Density (A/g)